The stability and transition of a two-dimensional jet

By HIROSHI SATO
Aeronautical Research Institute, University of Tokyo, Japan

(Received 23 April 1959)

A study was made of the transition of a two-dimensional jet. In the region where laminar flow becomes unstable, two kinds of sinusoidal velocity fluctuation have been found; one is symmetrical and the other is anti-symmetrical with respect to the centre line of the jet. The fluctuations grow exponentially at first and develop into turbulence without being accompanied by abrupt bursts or turbulent spots.

The response characteristics of laminar jets to artificial external excitation were investigated in detail by using sound as an exciting agent. The effect of excitation was seen to be most remarkable when the frequency of excitation coincides with that of self-excited sinusoidal fluctuations.

Numerical solutions of equation of small disturbances superposed on laminar flow were obtained assuming the Reynolds number as infinity. Theoretical eigenvalues and eigenfunctions are in good agreement with experimental results, thus verifying the existence of a region of linear disturbance in the two-dimensional jet.

1. Introduction

Theoretical investigations of the stability of boundary-layer-type flows are usually based on the assumption of a small disturbance. The fundamental equation is the well-known Orr–Sommerfeld equation, which has been solved under various boundary conditions.

In 1943, Schubauer & Skramstad (1948) verified the stability theory of laminar flow by their experiment on the boundary layer along a flat plate. The frequency, wave-number, amplification rate and amplitude function were in good agreement with theoretical predictions given by Tollmien, Schlichting and others. Since then, there has been little doubt concerning the validity of linearized theory, at least in the early stage of transition from laminar to turbulent flow.

Besides the boundary layer on a solid wall, there is another group of boundary layers. They are so-called 'free boundary layers', such as jets, wakes, separated layers, etc., in which the solid boundaries are absent in the flow field. The stability characteristics of free boundary layers are rather different from those of flows with a solid wall. The main reason for the difference seems to lie in the existence of a point of inflexion in the mean-velocity distribution of free boundary layers.

The laminar two-dimensional jet issued from a narrow slit was first investigated by Andrade (1939) using water. He found that when the Reynolds number was small, the observed mean-velocity distribution was in agreement with the theoretical 'similarity' solution. It was also pointed out that the jet became

unstable when the Reynolds number exceeded a certain value of the order of 10. The patterns of velocity fluctuations in a two-dimensional jet were clarified by the work of Brown (1935) in connexion with the sensitivity of jets to sound. His smoke pictures show vortex streets just like those observed in the wake of a cylinder. It was Savic (1941) who obtained an exact solution of the Orr–Sommerfeld equation for the two-dimensional jet. Although his solution was limited to the case of infinite Reynolds number, the wavelength and wave velocity of the oscillations were in good agreement with Brown's experimental results. Savic's comparison is, however, far from complete, because Brown did not give the mean-velocity distribution and Savic assumed that the observed pattern corresponded to neutrally stable fluctuations. More detailed numerical calculations of the wave-number and propagation velocity for various sets of the amplification rate of small oscillations were reported by Lessen & Fox (1955) in the case of infinite Reynolds number. Recently, Tatsumi & Kakutani (1958) have given the neutral curve for a wide range of Reynolds number. The present investigation was undertaken with the intention of comparing the experimental results with those existing theories. The first part of this paper gives measurements of the mean and fluctuating components of velocity in the transition region of two-dimensional jet. The next part describes some numerical solutions of the Orr–Sommerfeld equation, which were carried out after the above-mentioned theoretical work had been found unsatisfactory for comparison with the experiments, since the mean-velocity distribution assumed in the existing theories was not realized experimentally. In the final part, both experimental and theoretical results are compared, and the general features of transition of free boundary layers are discussed.

It was not intended to determine the critical Reynolds number for instability, since a completely different set of equipment was necessary for it. Experimental results for an air-jet at extremely low Reynolds number will be reported in the near future.

2. Experimental arrangement

2.1. *Two-dimensional jet*

The experiment was conducted on a jet issued from a rectangular slit. The general layout is shown in figure 1. The flow is accelerated from a settling chamber, passes through a parallel two-dimensional channel, and issues from a slit as a two-dimensional jet. The width $2h$ and the length l of the parallel channel were changed over five different sets of values in order to cover a wide range of Reynolds number as well as mean-velocity distribution at the slit. The breadth of the slit was 40 cm in all cases. The five combinations of width and length of channel used are tabulated in table 1. Detailed measurements were made using the combination of values denoted by SLIT 4·4 mm S and SLIT 6 mm L in table 1.

Air was supplied by an axial blower which was driven by a direct-current motor. The maximum wind-speed at the centre of the slit was 25 m/sec. Special care was taken to reduce disturbances at the test section. Velocity fluctuations were reduced by the use of a large settling chamber and damping screens. The ratio of the areas of settling chamber and two-dimensional channel was 67 for SLIT 6 mm L, for example, which was exceptionally large compared with the

contraction ratio of conventional wind-tunnels. The residual turbulence level at the slit was below 0·1%. Acoustic noise was also carefully reduced. The noise level at the test section was approximately 47 decibels, no predominant frequency component was found in the noise. Slight draught from windows and breeze due to the circulation of air inside the laboratory also tended to cause early transition of the jet. They were weak in the present experiments, but their effects were observed as a slow velocity fluctuation at the outer edge of the jet. The two-dimensional character of the jet was found to be satisfactory by checking the mean-velocity distribution.

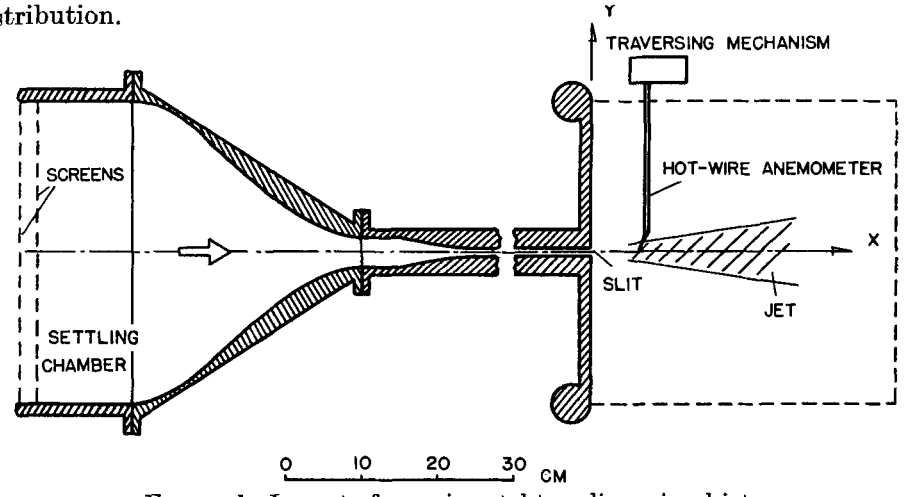

FIGURE 1. Layout of experimental two-dimensional jet.

Notation for experimental conditions	Width $2h$ (mm)	Length of channel l (mm)	Aspect ratio
SLIT 40 mm S	40	300	10
SLIT 10 mm S	10	300	40
SLIT 4·4 mm S	4·4	300	91
SLIT 10 mm L	10	1100	40
SLIT 6 mm L	6	1100	67

TABLE 1. Dimensions of channel and slit. The aspect ratio is the ratio of breadth to width of slit.

2.2. *Hot-wire equipment*

Hot-wire anemometers were exclusively used for measurements of both mean and fluctuating velocities. At first, a fine Pitot tube was used for the mean-velocity measurements. But when a large error was found due to the static-pressure variations across the layer and large inclination of flow in the transition region, all the data obtained by the Pitot tube were discarded.

Mean-velocity surveys by hot-wire were made for U and V, the longitudinal and transverse velocities (respective to the X- and Y-directions), while for the velocity fluctuations only the longitudinal component u was measured except in a few special cases. For the anemometers, use was made of 10% rhodium

platinum wire, 5μ in diameter and about 1·5 mm in length. Care was taken to prevent vibration of the wire. Characteristics of hot-wire anemometer at extremely low speed had previously been investigated in detail by the present author (1957); the calibration curve down to 20 cm/sec had been established, and errors occurring in the measurements in highly turbulent stream had been estimated. These results were fully utilized in the present investigation.

A full account of the electronic equipment may be found in a paper by Sato *et al.* (1954). The overall frequency response of hot-wire and amplifiers was flat from 20 to 20,000 c/s, provided the compensation was properly adjusted.

The hot-wire anemometers were traversed in the X- and Y-directions with micrometer screws. Accuracy of Y-positioning at different X-stations was approximately 0·1 mm, while relative position at the same X-station was read to within 0·01 mm by a precision dial-gauge. The accuracy of X-positioning was about 0·1 mm.

2.3. *Artificial excitations*

For the artificial excitation of fluctuations in the flow, use was made of a 10 W loudspeaker placed facing the test section. The intensity of sound was uniform throughout the test section and no noticeable resonance effect was detected in the frequency range from 30 to 800 c/s. The influence of the angle of incidence of the sound to the flow was very slight, but the direction of the sound was made perpendicular to the flow direction. The maximum intensity of sound from the loudspeaker was about 100 decibels including the background noise.

It was not attempted to determine the absolute intensity of sound exactly since the background noise changed from day to day and it was impossible to measure accurately the intensity of sound in the stream.

3. Experimental results

In this section, experimental data are presented without discussion. The comparison of experiment with theoretical results is deferred until § 5.

It should first of all be noted that the transition phenomenon was very unstable, that is, it was easily affected by various kinds of outside condition, for example, acoustic noise, draught, vibration, etc. In fact, the natural transition takes place as a result of the amplification of extremely small outside disturbances. These small disturbances change day by day and lie beyond our control. In spite of the careful arrangements described in § 2, the flow field in the transition region sometimes showed poor reproducibility. For this reason, an experimental accuracy of 10 % was the best attainable for certain measurements, while for most parts of the present experiments errors were expected to be of the order of 5 %.

3.1. *Natural transition*

The mean-velocity distribution in the laminar region of a jet depends on the condition upstream, that is, on the velocity distribution at the slit. When the length of channel l is long enough compared to the width $2h$ of the slit, the mean-velocity distribution at the slit is parabolic. On the other hand, when l is not large, the boundary layer on the wall of the channel is not thick enough to cover the whole cross-section; therefore the velocity distribution has a flat part at

the central region. Schlichting (1934) showed that the velocity distribution in the inlet region of laminar two-dimensional channel flow depends on a non-dimensional parameter $\nu l/h^2 U_{00}$, where ν is kinematic viscosity and U_{00} is the velocity at the centre of the slit. Measured mean-velocity distributions at the slit for various combinations of l, h and U_{00} were in good agreement with Schlichting's calculations.

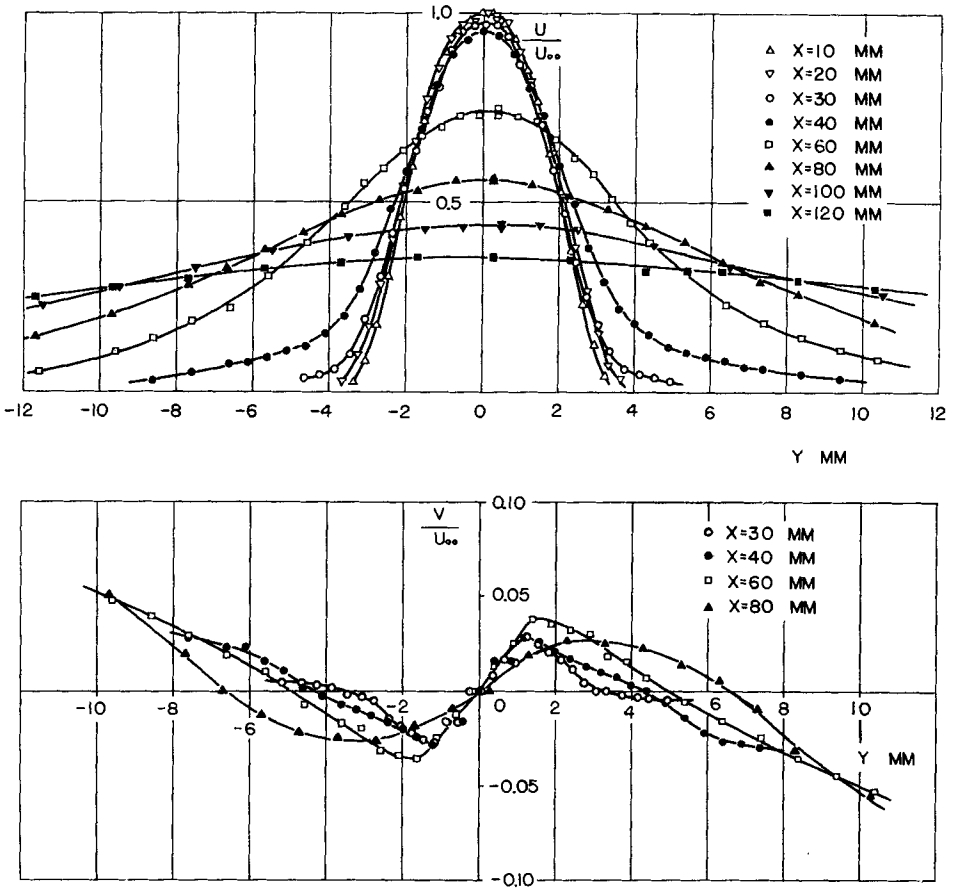

FIGURE 2. Mean-velocity distribution. SLIT 6 mm L, $U_{00} = 10{\cdot}0$ m/sec. X is measured from the slit.

Figure 2 shows an example of mean-velocity distribution for SLIT 6 mm L, $U_{00} = 10{\cdot}0$ m/sec and $\nu l/h^2 U_{00} = 0{\cdot}18$. In this case, the distribution at the slit is approximately parabolic. The variation of mean-velocity distribution with respect to the distance downstream is described as follows.

Before transition takes place, the change of distribution is gradual, except at the outer region of the jet, where the increase of velocity is very great due to the sudden change of boundary conditions there. At the central part, velocity changes quite little. At about 3 to 8 times of total width of channel downstream from the slit, depending on the initial distribution, the variation of distribution becomes very marked, that is, a large decrease of central velocity and rapid broadening

of the jet takes place. Further downstream, the mean-velocity distribution becomes similar, regardless of the initial velocity distributions.

In the same figure, the distribution of lateral mean velocity is also shown. The magnitude of V is rather small compared with U, except at the edge of jet. This fact justifies the neglect of V in the theoretical treatment.

The above-mentioned general trend is more clearly demonstrated in figures 3 and 4. In figure 3, the half breadth b (i.e. the distance from the centre line to the point where U/U_0 is 0·5, U_0 being the mean velocity at the centre line) is plotted against $X/2h$. It is shown that the development of breadth is gradual at first and becomes directly proportional to $X/2h$ as the distance downstream increases. The

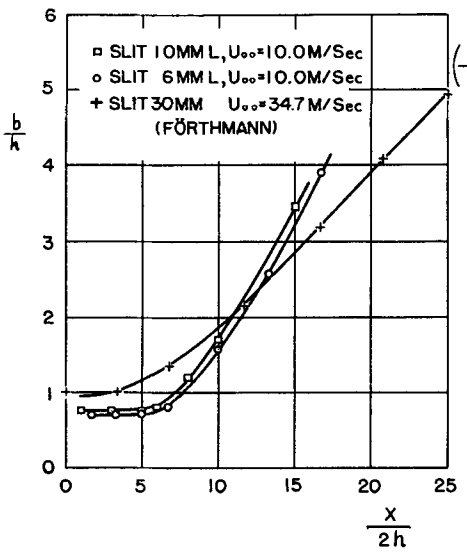

FIGURE 3. Spread of half breadth b of jet.

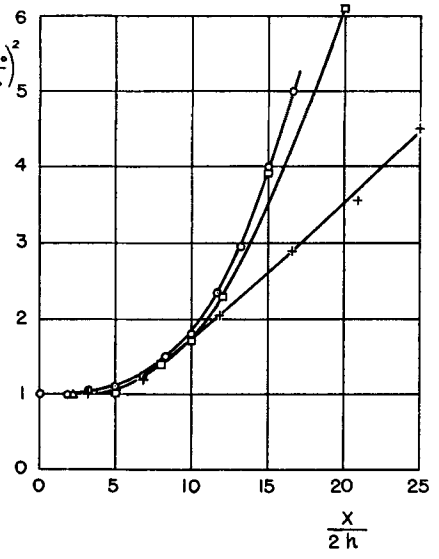

FIGURE 4. Variation of mean velocity on the centre line of jet.

experimental data of Förthmann (1934) are added. They show a tendency similar to the present results. In figure 4, the centre-line velocity U_0 is plotted in the form $(U_{00}/U_0)^2$ against $X/2h$. When $X/2h$ is small, U_0 stays approximately constant. As $X/2h$ increases, $(U_{00}/U_0)^2$ begins to increase and tends to become proportional to $X/2h$ when the distance downstream increases further. These linear relations seem to be characteristic of turbulent jet. The point of sharp rise of b/h or $(U_{00}/U_0)^2$ may correspond to the 'transition point'. The definition of the transition point is, however, quite arbitrary and the change from laminar to turbulent flow never takes place at a 'point'.

Figure 5 (plate 1) is a reproduction of oscillographic records of u-fluctuations at a small distance downstream from the slit. The wave-forms are nearly sinusoidal, higher frequency corresponding to higher wind-speed. At first, it was questioned that this regular pattern might be possibly caused by vibrations of the hot-wire anemometer or some kind of acoustical resonance in the channel. The former possibility was soon ruled out, since the change of hot-wire support caused no change in fluctuation patterns. The possibility of a resonance phenomenon was investigated by a small microphone. No distinct frequency component was found in the sound

at the test section and settling chamber. It was confirmed that transition of the jet is initiated by sinusoidal velocity fluctuations, which are weak at first and then amplified as the distance downstream increases. This was expected in view of the experiments on separated layers conducted by the present author (1956), because essential features of transition seem to be identical for both separated layer and jet. A remarkable difference, however, exists between the two. In the jet, two

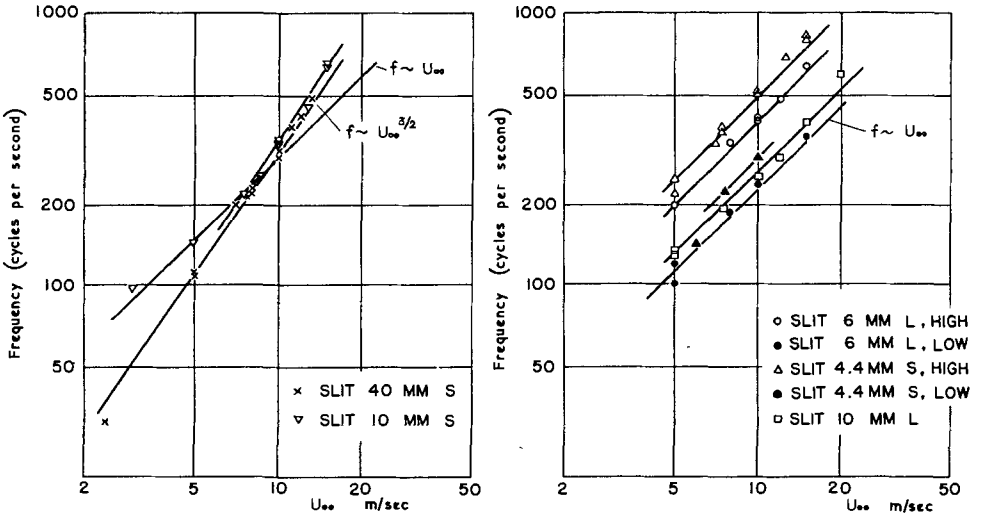

FIGURE 6. Frequency of sinusoidal velocity fluctuations plotted against central velocity at the slit U_{00}.

modes of fluctuation are found. They are different in frequency as well as in phase relation. Fluctuations shown in figure 5(A) are at higher frequency and are symmetrical with respect to the centre-line, while fluctuations shown in figure 5(B) are at lower frequency and are anti-symmetrical. In the separated layer, only one mode of fluctuation exists. The relative intensity of two modes of fluctuation is strongly dependent on the mean-velocity distribution. When $\nu l/h^2 U_{00}$ is large at the slit, i.e. the velocity distribution is nearly parabolic, the anti-symmetrical fluctuation prevails. On the other hand, when $\nu l/h^2 U_{00}$ is small, the anti-symmetrical fluctuation is not observed.

In figure 6, the fluctuation frequency is plotted against wind-speed. When the slit is wide, the frequency is approximately proportional to the $\frac{3}{2}$ power of wind-speed, as in the case of a pure separated layer (Sato 1956). A similar relation between frequency and wind-speed was found by Wehrmann & Wille (1957) for a circular jet. On the other hand, when the slit is narrow, as shown in the right half of the figure, the frequency is proportional to the wind-speed. These facts suggest that the frequency depends on the thickness of the shear layer rather than the width of the slit. When the slit is narrow, the velocity distribution at the slit is parabolic, and then the thickness of shear layer does not depend on the wind-speed; while for the wider slit, the thickness of shear layer is inversely proportional to the square root of wind-speed as in the case of a separated layer. This may explain the difference in the relation between frequency and wind-speed for different sizes of slit.

Simultaneous records of u-fluctuations at two different points separated in the X-direction revealed that the sinusoidal fluctuation is a progressive wave in the X-direction.

Figure 7 shows the energy spectrum of the u-fluctuations in the region where sinusoidal fluctuations are found. The scale of the ordinate is chosen arbitrarily, but the relative magnitude of two curves is represented correctly. At $Y = 0$, there is a single peak corresponding to the symmetrical fluctuations; while at $Y = 2$ mm, two peaks are observed at high and low frequencies.

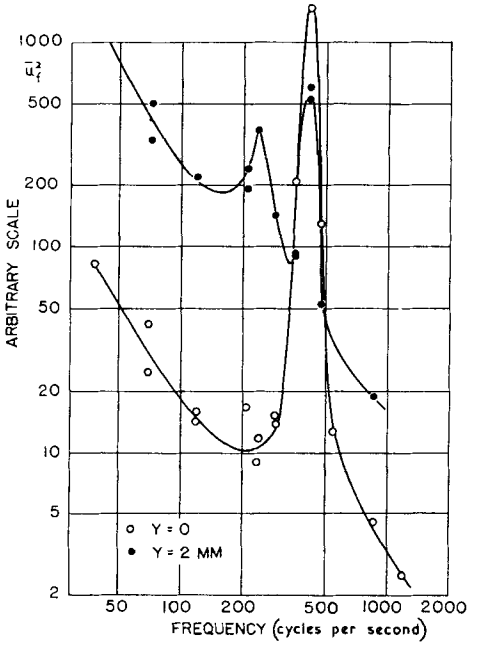

FIGURE 7. Energy spectrum of u-fluctuations. SLIT 6 mm L, $U_{00} = 10{\cdot}0$ m/sec, $X = 30$ mm.

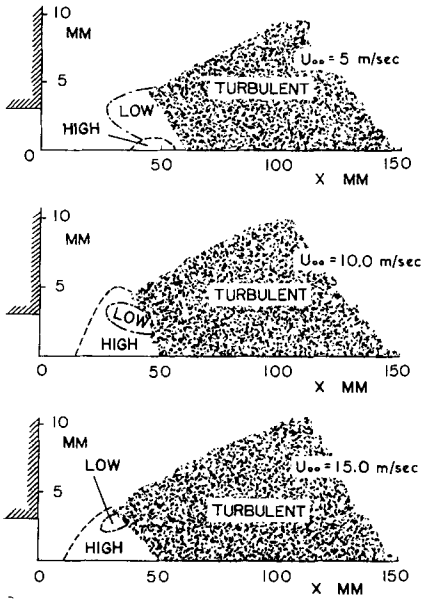

FIGURE 8. Map of patterns of u-fluctuations. SLIT 6 mm L.

After the existence of sinusoidal fluctuation was confirmed, a complete survey of the u-fluctuations was made in the transition region. Results of detailed observations of patterns of u-fluctuation are summarized in figure 8 as a map of various fluctuation patterns. Inside regions denoted by *HIGH* or *LOW*, sinusoidal fluctuations of high frequency (symmetrical) or low frequency (anti-symmetrical) are observed. It is shown that the extent of the region where there are two types of sinusoidal fluctuation depends on wind-speed—or more precisely, on mean-velocity distribution.

Wave-forms of the u-fluctuations at various X- and Y-positions are reproduced as figure 9 (plate 2). No marked bursts of turbulence are found in the wave-form. Development from sinusoidal into irregular fluctuation is gradual. Some intermittent bursts are observed only at the outer edge of the turbulent jet.

The distribution of the u-fluctuations is shown in figure 10, with SLIT 6 mm L and $U_{00} = 10{\cdot}0$ m/sec. The distribution is almost similar when X is small, and positions of peaks in the distribution approximately coincide with positions of maximum gradient in mean-velocity distribution. As the distance downstream

increases, values at peak and bottom become closer. The root-mean-square intensity, expressed as a ratio to U_{00}, reaches its maximum at about $X = 80$ mm and then decreases gradually. This is more clearly shown in figure 11, in which the

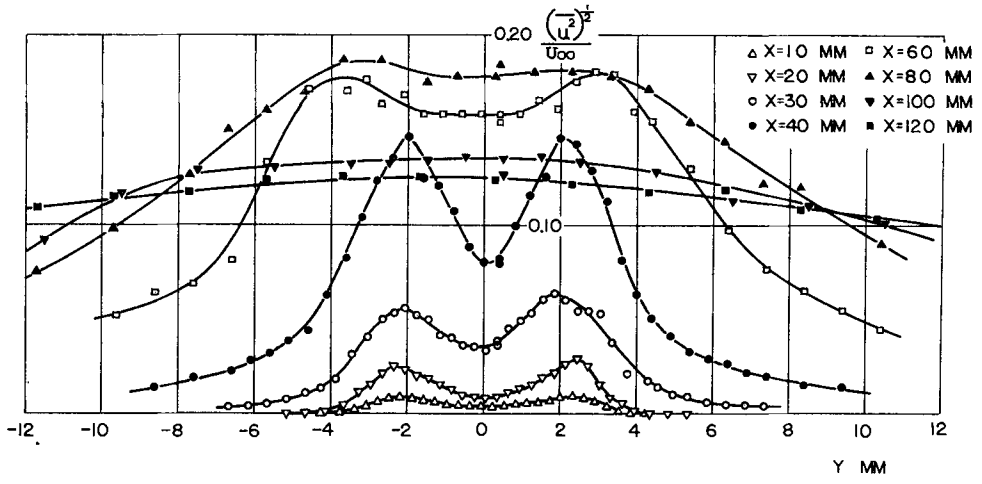

FIGURE 10. Distribution of intensity of u-fluctuations.
SLIT 6 mm L. $U_{00} = 10{\cdot}0$ m/sec.

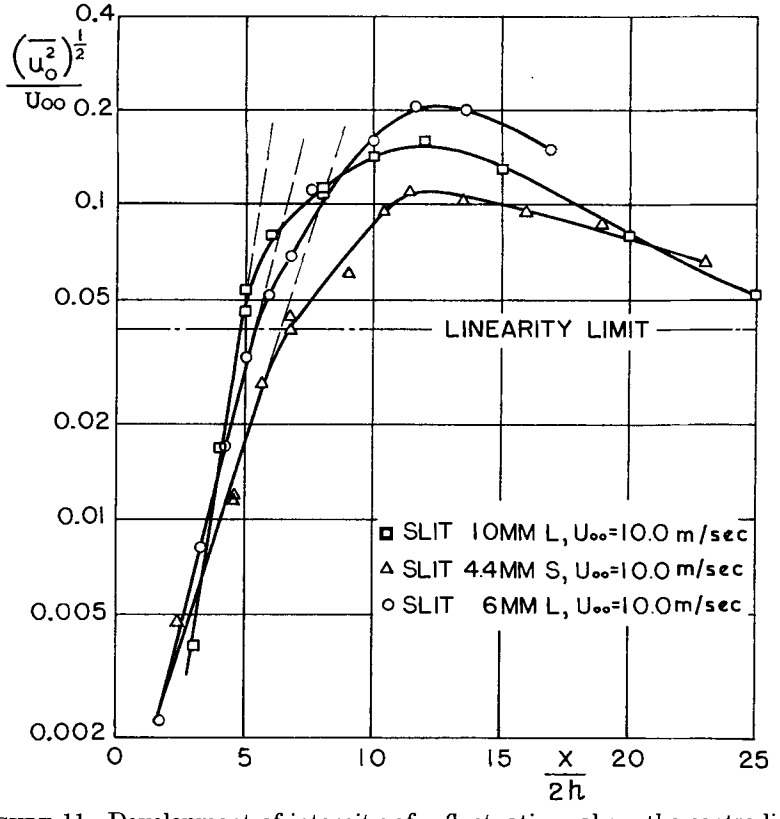

FIGURE 11. Development of intensity of u-fluctuations along the centre line in a logarithmic plot.

intensity on the centre line is plotted against $X/2h$. Three curves for three different sizes of slit indicate an identical general trend. In the logarithmic plot, the intensity on the centre line increases linearly, in other words, grows exponentially when $X/2h$ is small. When the intensity reaches approximately 0·04, the rate of growth becomes less and the maximum value appears at about $X/2h = 12$. This general trend suggests the possibility of classifying fluctuation field into two parts. Points on the X-axis where $(\overline{u^2})^{\frac{1}{2}}/U_{00} = 0{\cdot}04$—denoted as *LINEARITY LIMIT*—distinguish the region of exponential growth from non-exponential region. It is worth while to note that the point where the sharp increase of breadth of the jet takes place approximately coincides with the above-mentioned dividing point.

3.2. *Excited transition of jet*

The sound from the loudspeaker proved to be satisfactory as a means of artificial excitation. It had, however, some shortcomings. First, the sound could not be focused, so the excitation was distributed over the flow field. And

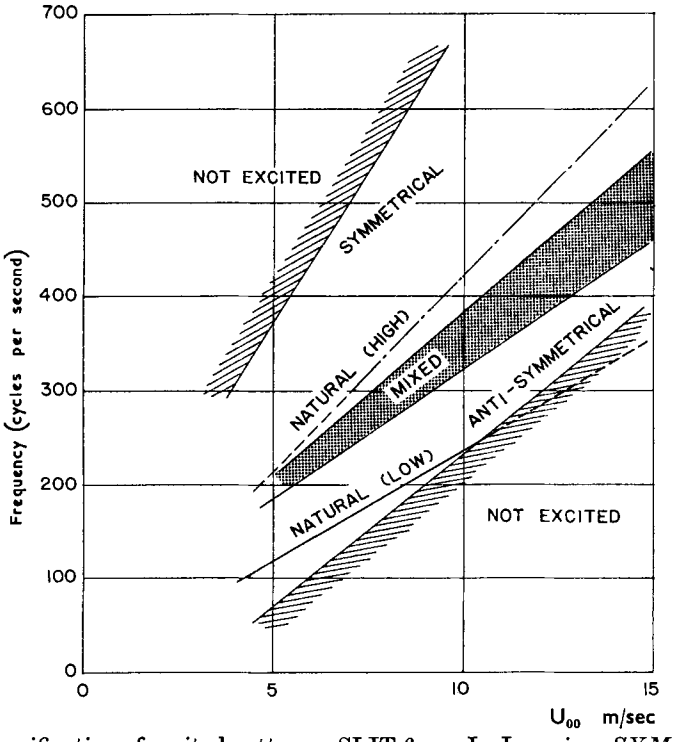

FIGURE 13. Classification of excited patterns. SLIT 6 mm L. In regions *SYMMETRICAL* and *ANTI-SYMMETRICAL*, symmetrical and anti-symmetrical sinusoidal velocity fluctuations are induced, respectively.

moreover, the relation between intensity of sound and velocity fluctuation is not fully understood in shear flows. Schubauer & Skramstad (1948) have pointed out that the effect of reflexion of sound from the tunnel wall can be fatal to a quantitative experiment. Fortunately, in the case of a jet, the flow field is open, and no effects of reflexion and resonance were found.

Before quantitative data are presented, some illustrative records of u-fluctuations are shown in figures 12 to 15. Figure 12 (plate 3) shows the effect of excitation on the u-fluctuations. Definite effects are found when the frequency of excitation is 390 or 420 c/s. In these cases, the frequency of induced velocity fluctuation is the same as that of the incoming sound. On the other hand, for lower (290 c/s) frequencies, the effect of excitation is hardly observed. It is thus confirmed that the rate of amplification strongly depends on the frequency of excitation. Results of systematic observations on this point are shown in figure 13. The limit of excitation, though it cannot be rigorously defined, varies approximately linearly with the wind-speed. In the region denoted by *MIXED*, both symmetrical and anti-symmetrical fluctuations are possible. Fluctuations excited by sound of higher frequency are symmetrical, while those by lower frequency are anti-symmetrical. Simultaneous records at $Y = 0$ and 2 mm with artificial excitations are reproduced as figure 14 (plate 3). With excitation of lower frequency (300 c/s), the amplitude of fluctuation is nearly zero at $Y = 0$, and with higher frequency (510 c/s), the fluctuation vanishes at $Y = 2$ mm.

The symmetricity of excited fluctuation is more clearly shown by the Lissajous figures in figure 15 (plate 4). Without excitation, the symmetrical fluctuation at high frequency is accompanied with anti-symmetrical fluctuation at low frequency. With excitations of 240 c/s and 330 c/s, the two signals are in adverse phase. At 330 c/s, the Lissajous figure is somewhat curved. With excitation at 420 c/s, the fluctuation is purely symmetrical, and at 600 c/s, the two modes are mixed. The figures at $Y = 2$ mm and 4 mm are completely different. Signals with excitation at 240 c/s are in the same phase and those excited at 420 c/s are almost in adverse phase.

It is apparent that there is a selective mechanism governing the two modes of fluctuation according to the frequency of excitation.

Effects of excitation on the mean velocity and intensity of fluctuation are shown in figures 16 to 18. It is noticed that the effect of excitation depends on its intensity. The background acoustic noise is around 47 decibels, and the following measurements were made with a sound intensity about 85 decibels including background noise. When the intensity of excitation is small, the effect is small, and at about 85 decibels the effect reaches its maximum and no longer increases with the increased intensity of excitation.

As shown in figure 16, effects on the mean velocity are not remarkable except at the outer part of jet. The increase of mean velocity there may be due to the increased intensity of fluctuation by excitation as shown in figure 17, which demonstrates the lateral distribution of intensity of fluctuation with and without excitations. The effect is remarkable again at 420 c/s. With this frequency, the wave-form of fluctuation is purely sinusoidal in the whole region of Y. The irregular slow fluctuation at the outer part of jet is suppressed, and a sinusoidal wave-form is observed even at $Y = 4$ mm. The phase inversion exists at about $Y = 3$ mm. With excitation at 330 c/s, which frequency is inside the region denoted by *MIXED* in figure 13, the intensity of fluctuation increases without changing the form of distribution. On the development of fluctuation along the centre line, effect of excitation is remarkable again when the frequency of sound

coincides with that of self-excited velocity fluctuation. This fact is conceivable since in a natural transition a sinusoidal fluctuation is supposed to be the disturbance which receives the maximum amplification. In figure 18, the intensity

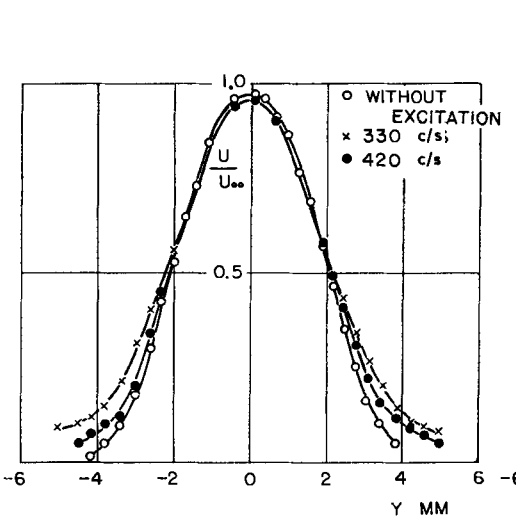

FIGURE 16. Effect of excitation on mean-velocity distribution. SLIT 6 mm L, U_{00} = 10·0 m/sec, X = 30 mm.

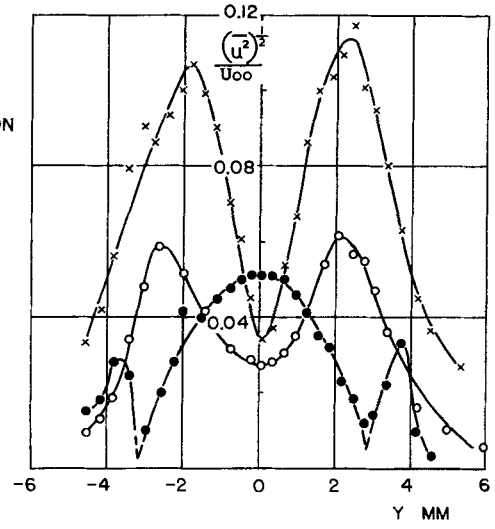

FIGURE 17. Effect of excitation on intensity of u-fluctuations. SLIT 6 mm L, U_{00} = 10·0 m/sec, X = 30 mm.

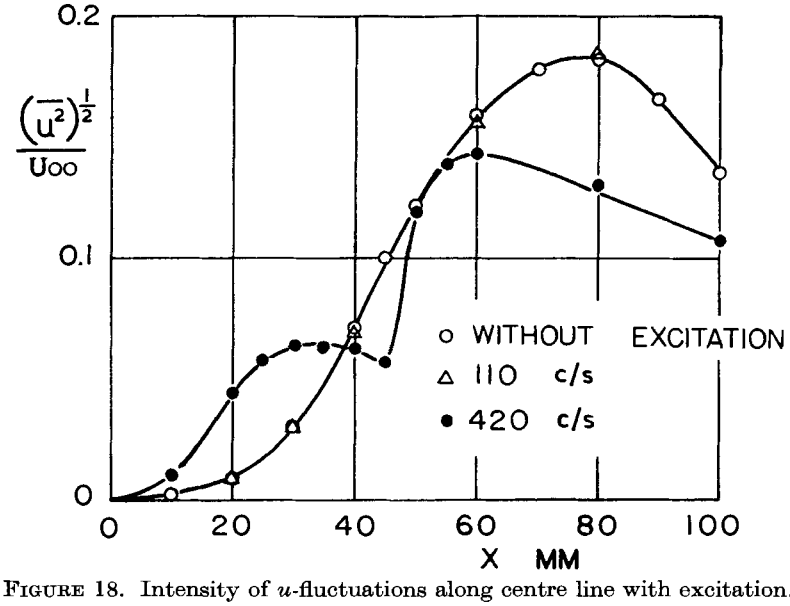

FIGURE 18. Intensity of u-fluctuations along centre line with excitation. SLIT 6 mm L, U_{00} = 10·0 m/sec.

of fluctuation with excitation at 420 c/s has two maxima along the centre line. With excitation at 110 c/s, the effect of excitation is hardly recognized.

Distributions of spectral components of the u-fluctuations are shown in figure 19 in which $(\overline{u_f^2})^{\frac{1}{2}}$ is the root-mean-square value of spectral components. The maximum value of $(\overline{u_f^2})^{\frac{1}{2}}$ is taken as unity. In the upper two curves, the 180-degree

phase shift is observed at $Y = 0$, and with excitation at 330 c/s, another phase inversion is probable at $Y = 3{\cdot}3$ mm. In the case of a filter setting at 420 c/s, no excitation was applied because the intensity of the component at 420 c/s is rather large even without excitation. A large phase shift seems to take place at about $Y = 3$ mm.

The development of spectral components on the X-axis is shown in figure 20. The scale of the ordinate is taken arbitrarily for components of different frequency,

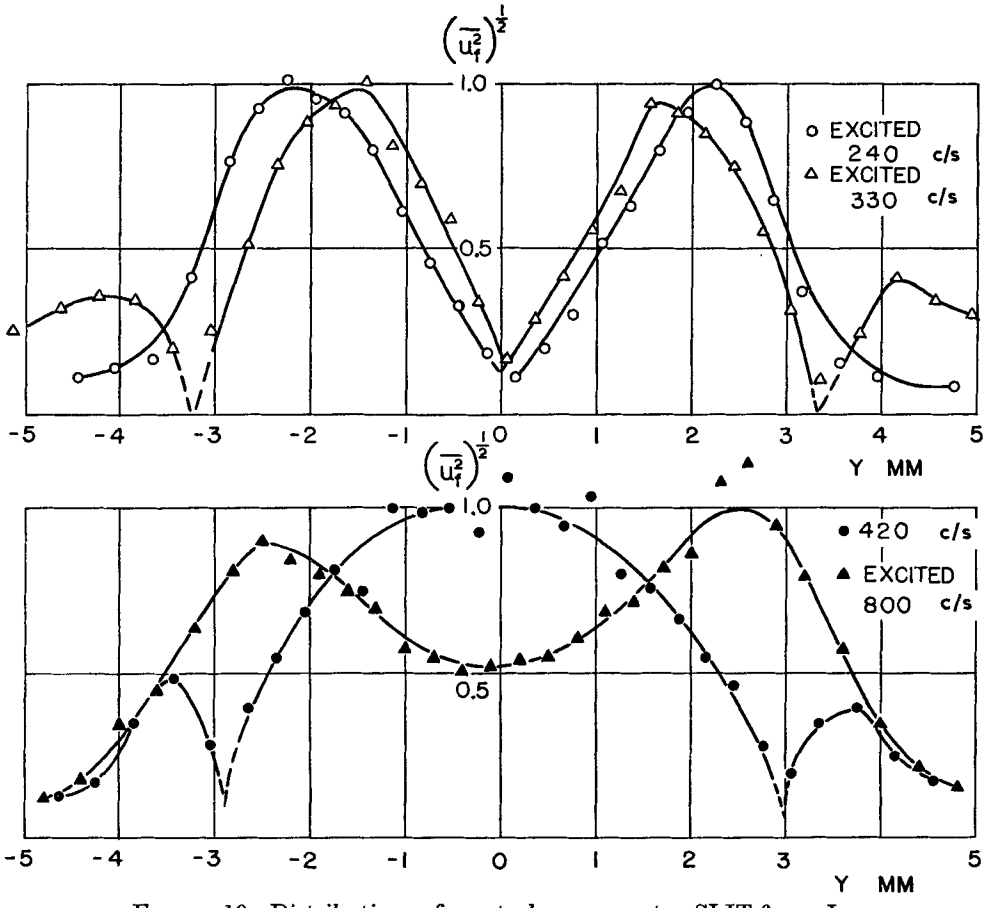

FIGURE 19. Distributions of spectral components. SLIT 6 mm L, $U_{00} = 10{\cdot}0$ m/sec, $X = 30$ mm.

while for the same frequency, the relative magnitude is correctly expressed. The intensity grows exponentially until it reaches the *LINEARITY LIMIT* which was explained above. Generally speaking, the growth rate deviates from being exponential earlier due to the presence of excitation. This is remarkably shown at the frequency 420 c/s. The exponential growth in this case is maintained only until $X = 20$ mm. From the gradient of each curve, the rate of amplification was calculated.

The damped fluctuation is not found in figure 20. In order to observe the damped fluctuation, the initial disturbance must be fairly large. Sound cannot

produce such a large disturbance at a specified point in the flow. In figure 21, the ratio of spectral components with and without excitation is plotted against frequency. The neutral frequency is determined as the point where the ratio becomes unity. Arrows under abscissa indicate the theoretical predictions which are described in detail in the next section.

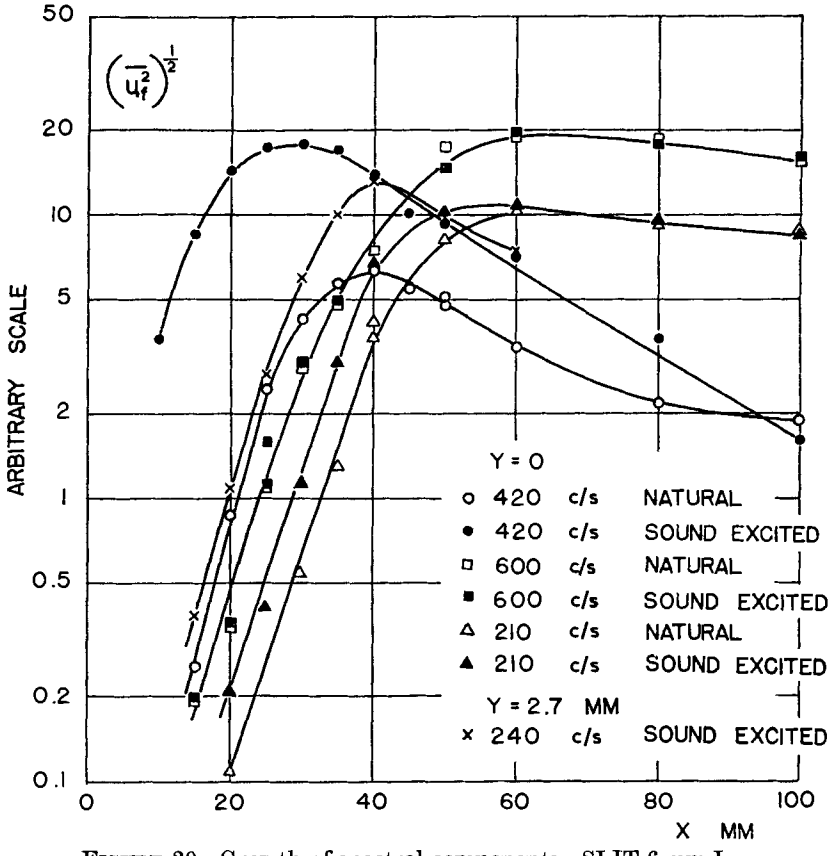

FIGURE 20. Growth of spectral components. SLIT 6 mm L, $U_{00} = 10{\cdot}0$ m/sec.

4. Theoretical considerations

The theoretical results on stability of two-dimensional jet obtained by Savic (1941) and others are found to be inadequate for the comparison with the present experiment, the main reason being the disagreement between the mean-velocity distribution assumed theoretically and the experimental one. In the theoretical work conducted so far, the basic flow was assumed to have the form $\mathrm{sech}^2 y$. This is the similarity solution for a fully developed laminar jet, but the transition usually takes place before this similarity distribution is established. This distribution may be realized before transition only when the Reynolds number is extremely low. The present experiments were made in the region of fairly high Reynolds number.

The work by Tatsumi & Kakutani (1958) shows that in the jet the wave-number of neutral oscillation varies little with Reynolds number if it is fairly

high. From this fact, we expect that the stability characteristics at high Reynolds number may well be approximated by those at infinite Reynolds number. Therefore, in this section Reynolds number is assumed infinity. Calculations are based on the Orr–Sommerfeld equation with various kinds of mean-velocity distribution which approximate the distribution obtained experimentally.

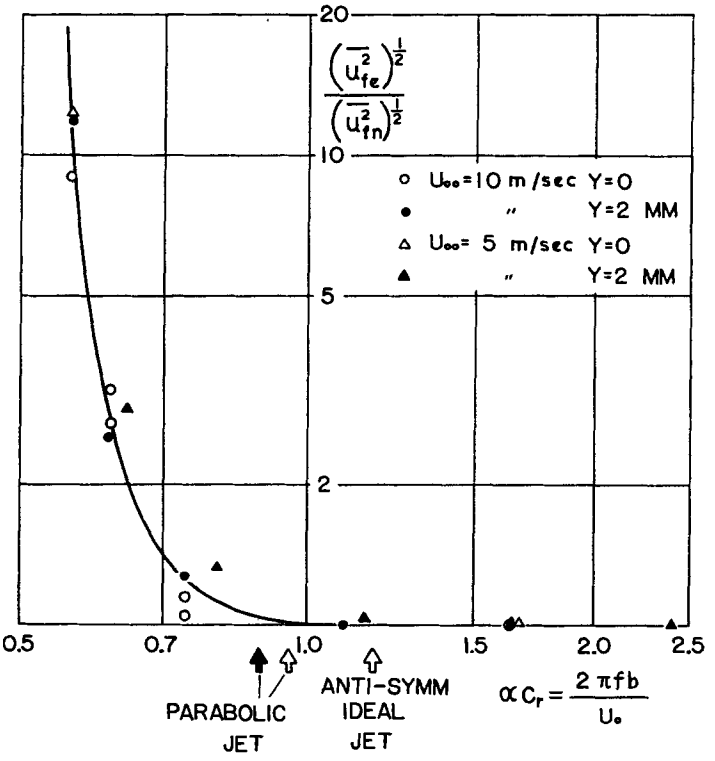

FIGURE 21. Determination of frequency of neutral oscillation. SLIT 6 mm L. $(\overline{u_{fe}^2})^{\frac{1}{2}}$ and $(\overline{u_{fn}^2})^{\frac{1}{2}}$ denote root-mean-square values of the components of frequency f with and without artificial excitation respectively.

4.1. *Mean-velocity distributions*

The mean-velocity distribution in the channel is characterized by a non-dimensional parameter vl/h^2U_{00} as mentioned before. The velocity distribution in a laminar jet is determined by the distribution at the exit of the channel and is, therefore, also characterized by vl/h^2U_{00}. As far as the jet remains laminar, the velocity distribution may approach to the similarity distribution of the form $\mathrm{sech}^2 y$.

From the above considerations, the following expression for the velocity distribution seems reasonable:

$$\frac{U}{U_0} = \left[1 + sky^2\left(\frac{2-y^2-y^4}{1+ky^6}\right)\right]\mathrm{sech}^2 ay, \tag{1}$$

in which y is the lateral distance non-dimensionalized by the half-breadth b, k and s are parameters which characterize the distribution and $a = 0{\cdot}88136$ is a constant.

Expression (1) was obtained from purely geometrical considerations. The

second term in the bracket is the modification from the similarity distribution and is chosen to make the best fit to the experimental distribution. At the central part of jet, expression (1) should approximate the velocity distribution in the inlet region of the channel. The parameter s is chosen as 0·7 to obtain the best fit at large y.

Four typical distributions used for the calculations are shown in figure 22. Parameters for each distribution are tabulated in table 2.

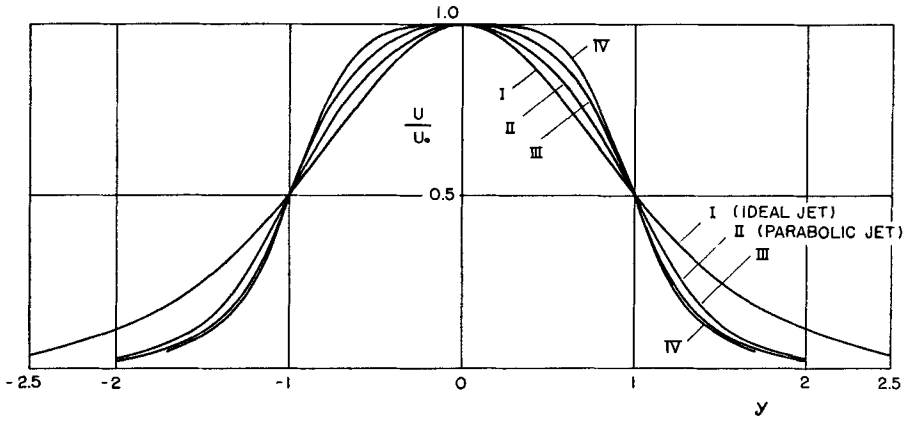

FIGURE 22. Theoretical mean-velocity distributions in jet used as basic flows for the calculation of small disturbances.

Notation	k	s	$U''(0)/U(0)$	Corresponding $\nu l/h^2U_{00}$	θ/b	Named
I	0	—	−1·5536	—	0·375	Ideal jet
II	0·1977	0·7	−1·0000	∞	0·255	Parabolic jet
III	0·3821	0·7	−0·4837	0·043	0·220	—
IV	0·5549	0·7	0	0·024	0·196	—

TABLE 2. Mean-velocity distributions used for the calculation of small disturbances.

4.2. *Disturbance equations*

The procedure of calculation presented here is one commonly employed. The basic flow is two-dimensional and is assumed to be a function of y only. The lateral velocity V is neglected. The disturbance velocities u and v are assumed to be functions only of x and y and of time. Quantities in the equations of motion and continuity are made non-dimensional by taking the half-breadth b and central velocity U_0 as units, these being assumed not to vary with x in the following theory.

Since u and v are small, the disturbance equations are linearized as the Orr–Sommerfeld equation, that is,

$$\left(\frac{U}{U_0}-c\right)(\phi''-\alpha^2\phi)-\frac{U''}{U_0}\phi=\frac{1}{i\alpha R}(\phi^{\mathrm{IV}}-2\alpha^2\phi''+\alpha^4\phi) \qquad (2)$$

in which primes mean differentiation with respect to y. The function ϕ is defined as follows: if u and v are expressed in terms of a stream function ψ as

$$u=\partial\psi/\partial y, \quad v=-\partial\psi/\partial x,$$

then ψ is written as

$$\psi = \phi(y) \exp[i\alpha(x-ct)]. \tag{3}$$

Here α is the wave-number and c is usually complex in the form $c = c_r + ic_i$, in which c_r is the propagation velocity and c_i is a measure of the rate of amplification of disturbances.

When the Reynolds number $R = bU_0/\nu$ is very large, we have approximately

$$\left(\frac{U}{U_0} - c\right)(\phi'' - \alpha^2\phi) - \frac{U''}{U_0}\phi = 0. \tag{4}$$

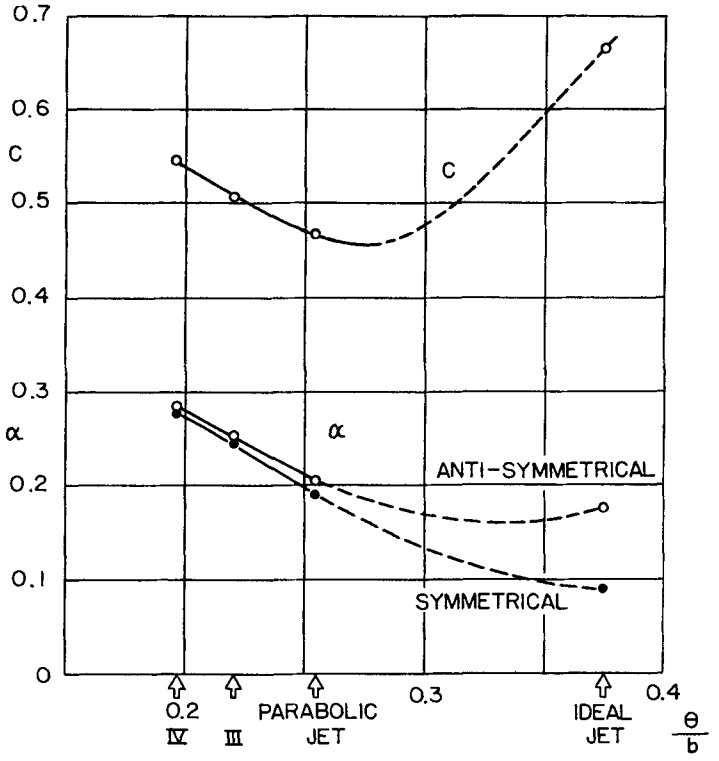

FIGURE 23. Propagation velocity c and wave-number α of neutral oscillations for various kinds of mean-velocity distribution.

The justification for using equation (4) in place of (2) is based on the fact that the stability characteristics of jet-type flows are insensitive to Reynolds number if it is high, in contrast with the case of flow with solid boundaries.

The solution of equation (4) was obtained by numerical integrations using the Runge–Kutta procedure.

4.3. *Neutral oscillations*

If $c_i = 0$, the disturbance is neither amplified nor damped. For the neutral oscillation, it is known that when the basic flow has an inflexion point in the velocity distribution, the propagation velocity c_r is equal to the mean velocity at the inflexion point. Thus, c_r is easily determined for each mean-velocity distribution from I to IV.

Boundary conditions for determining α and ϕ are, because of the symmetricity of basic flow,

$$\text{at} \quad y = \pm\infty, \quad \phi, \phi' \quad \text{are bounded;}$$

$$\text{at} \quad y = 0, \begin{cases} \phi = 0, & \phi' = 1 \quad \text{for symmetrical disturbances,} \\ \phi = 1, & \phi' = 0 \quad \text{for anti-symmetrical disturbances.} \end{cases}$$

The numerical integration was started at $y = 0$ and proceeded along the real axis, and was repeated until the boundary condition at large y was satisfied.

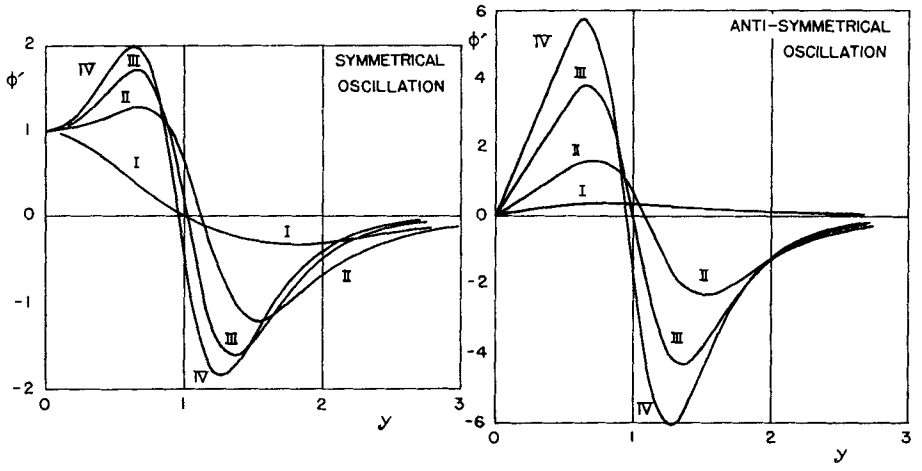

FIGURE 24. Amplitude function of neutral oscillations.

In figure 23, the propagation velocity and wave-number are plotted against θ/b, in which θ is the momentum thickness defined by

$$\theta = \int_0^\infty \frac{U}{U_0}\left(1 - \frac{U}{U_0}\right) dY.$$

θ/b is a form parameter which expresses the flatness of the mean-velocity distribution. θ/b is 0·375 for ideal jet and zero if the thickness of shear layer is zero compared with the breadth of jet. When θ/b is small, α is nearly the same for symmetrical and anti-symmetrical oscillations.

Figure 24 shows the calculated amplitude function ϕ' which expresses the u-fluctuation. The change of sign means a phase reversal at the point.

4.4. *Amplified oscillations*

When $c_i > 0$, the disturbance is amplified. Variables in equation (4) are complex and eigenvalues α, c_i and c_r are unknown. Equation (4) is separated into real and imaginary parts and integrated along the real axis with appropriate boundary conditions.

Figure 25 shows the values of α and c_i as a function of c_r on the parabolic jet (distribution II). Small circles denote calculated values. A great difference is seen for different mean-velocity distributions.

Before we compare these theoretical results with experiment, we have to make a transformation of time axis and X-axis by the relation

$$x = c_r t,$$

since the flow is stationary and the disturbance is amplified when it travels in the X-direction. Thus the spatial rate of amplification is $\alpha c_i/c_r$ instead of c_i.

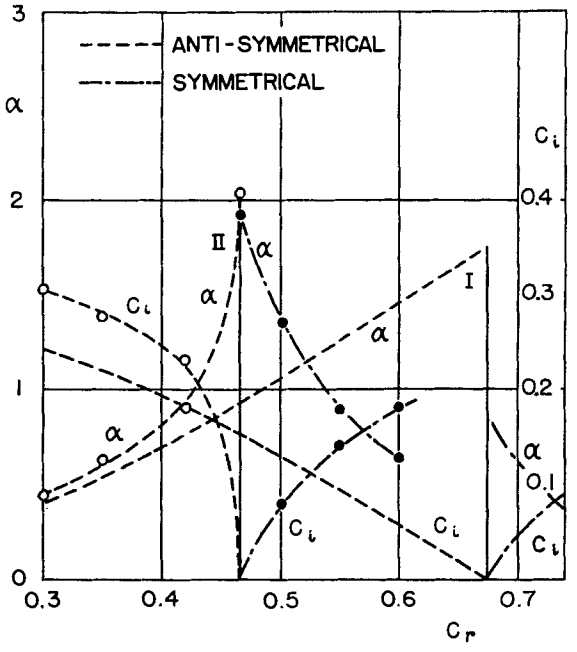

FIGURE 25. Wave-number α and amplification rate c_i of amplified oscillations.

5. Discussion

5.1. *Mean-velocity distribution*

The non-dimensional plot of mean-velocity distribution is shown in figure 26 in which $\nu l/h^2U_{00} = 0{\cdot}18$. It is apparent that for small values of X, the distribution is well approximated by curve II rather than I. Since, in this case, the sinusoidal velocity fluctuation is observed around $X = 20$ to 30 mm, the ideal jet is apparently not adequate as the basic flow for discussing the nature of small disturbances.

When the value of $\nu l/h^2U_{00}$ is smaller, the mean velocity has a flat distribution at the central core, and distributions III and IV well approximate cases where $\nu l/h^2U_{00} = 0{\cdot}043$ and $0{\cdot}024$, respectively. As a limiting case, when $\nu l/h^2U_{00} = 0$, the jet is really a separated layer.

At this point in the work, it was questioned that this kind of observed mean-velocity distribution might possibly be the result of a particular geometrical shape of slit. Since it seemed possible to change the distribution by modifying the shape of slit, measurements were carried out either making the edge of slit round or attaching small pieces to make the edge of slit sharper. These changes, however, little affected the distribution, and the ideal jet (distribution I) was not realized experimentally. Therefore, we returned to the 90°-edge slit because it is well defined. The reason why Andrade (1939) observed the ideal-jet distribution may have been due to the low Reynolds number in his experiment.

5.2. *Frequency of sinusoidal fluctuations*

The frequency of sinusoidal fluctuations in the jet has no simple relation with wind-speed. Figure 27 is a non-dimensional plot of frequency based on the total width of slit $2h$ and central speed U_{00}. The number $S_j = 2hf/U_{00}$ corresponds to the

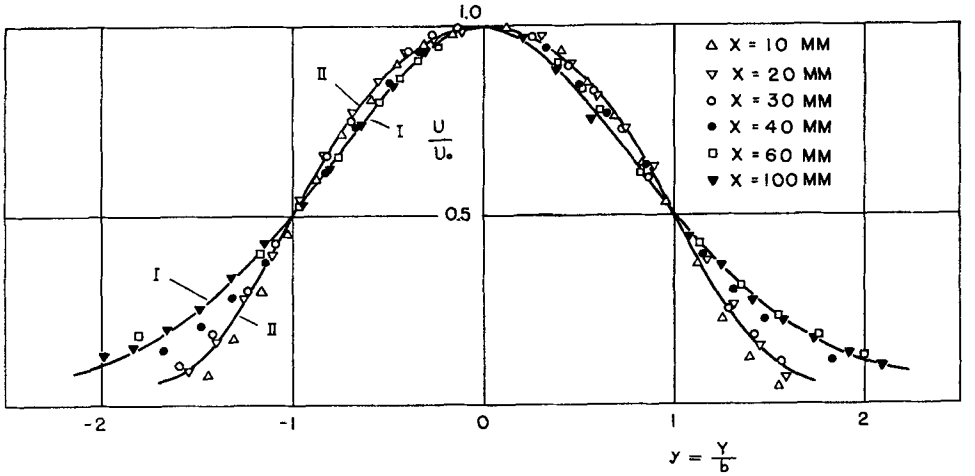

FIGURE 26. Non-dimensional plot of mean-velocity distribution. SLIT 6 mm L, $U_{00} = 10{\cdot}0$ m/sec.

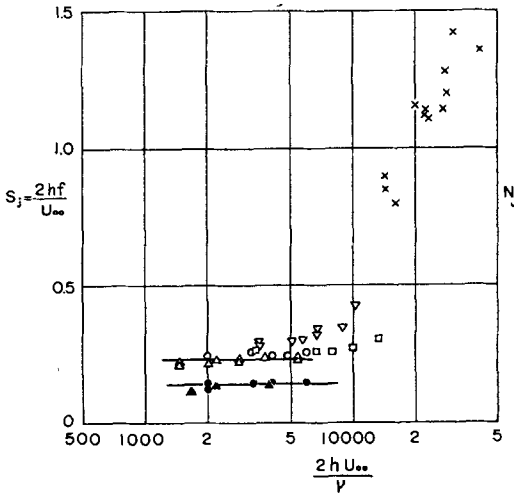

FIGURE 27. Frequency of sinusoidal velocity fluctuations, non-dimensionalized by the total width of slit $2h$.

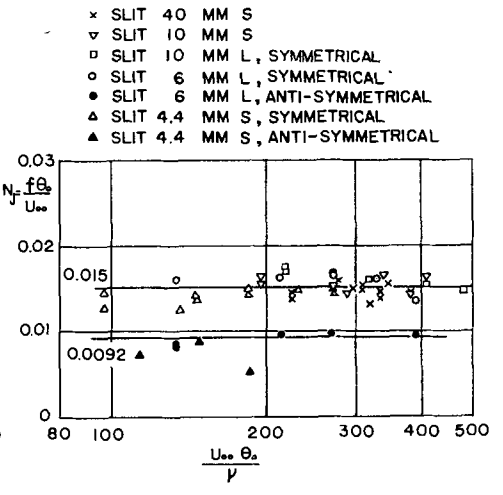

FIGURE 28. Non-dimensional frequency based on the momentum thickness at slit θ_0.

Strouhal number for the wake of a cylinder. Values of S_j for various Reynolds numbers are far from constant, except in the region of small Reynolds number. In the present series of experiments, vl/h^2U_{00} was large when the Reynolds number was small. In the Reynolds number range from 1500 to 8000, the mean-velocity distribution at the slit is parabolic; therefore the characteristic length remains

unchanged with U_{00}. This fact results in the constant value $S_j = 0{\cdot}23$ for symmetrical fluctuations and 0·14 for anti-symmetrical fluctuations.

In order to obtain more general relation between the fluctuation frequency and U_{00}, the momentum thickness of layer is a more suitable characteristic length than the width of slit. In figure 28, a new non-dimensional number $N_j = f\theta_0/U_{00}$ is plotted against the Reynolds number, θ_0 being the momentum thickness in one side at the slit. N_j is almost constant, and moreover it has the same value 0·015 for symmetrical fluctuation of higher frequency as shown in the separated layer (Sato 1956).

5.3. *Comparison with linearized theory*

The comparison of the experimental results with linearized theory is shown in figures 29 to 32. Experimental data used for the comparison are those with large values of $\nu l/h^2U_{00}$.

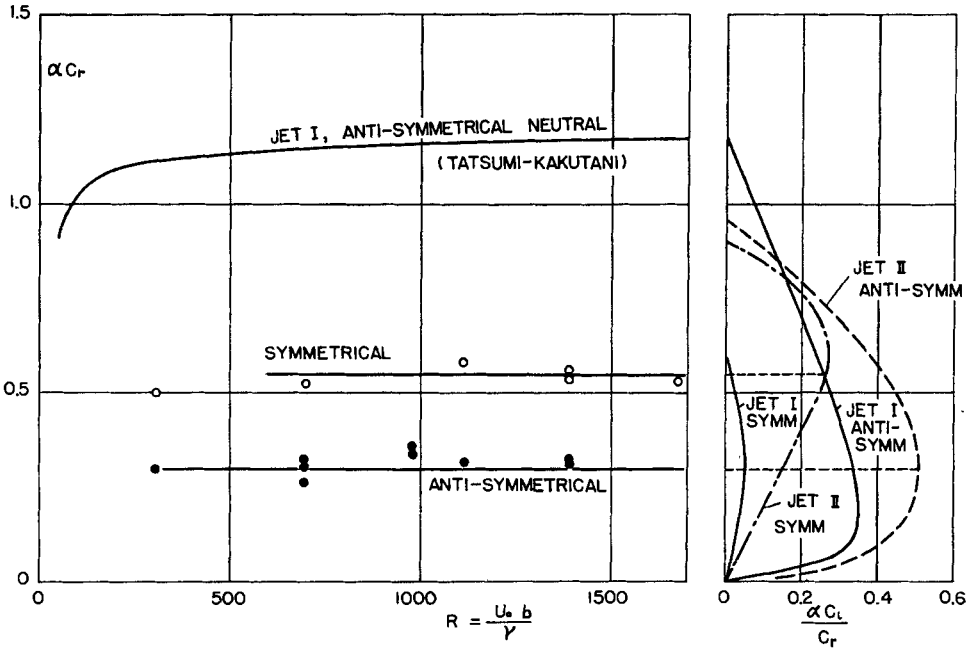

FIGURE 29. Comparison of theoretical and experimental results. Frequency of velocity fluctuation $\alpha c_r = 2\pi f b/U_0$.

Figure 29 shows the comparison of frequency non-dimensionalized by the half-breadth b and central speed U_0. In the right of the figure, theoretical results for the spatial rate of amplification $\alpha c_i/c_r$ at infinite Reynolds number are shown. The observed frequency is expected to correspond to that with maximum rate of amplification. Theoretical results by Lessen & Fox (1955) taking the ideal jet (Jet I) as a basic flow show no correlation with the experimental results. On the other hand, calculations in the preceding section based on the parabolic jet (Jet II) verifies the above statement, namely, that the frequency of sinusoidal fluctuation found in natural transition corresponds to the frequency of the small disturbance which receives maximum spatial rate of amplification theoretically.

The neutral curve given by Tatsumi & Kakutani gives the limit for the existence of amplified fluctuations in the ideal jet.

Figure 30 shows a comparison concerning the propagation velocity of artificially excited sinusoidal fluctuations. Generally speaking, the experimental points are closer to theoretical results for the parabolic jet (Jet II) than those for the ideal jet, and the agreement of both theoretical and experimental results is considered to be satisfactory.

Figure 31 shows the spatial rate of amplification $\alpha c_i/c_r$ plotted against frequency αc_r. For symmetrical fluctuations, experimental values for $\alpha c_i/c_r$ are almost twice and for anti-symmetrical fluctuations 4/5 times the theoretical results for the parabolic jet (Jet II). The reason for this discrepancy may be the slight misfit of assumed mean-velocity distribution, or may be due to the pressure gradient in the region of sinusoidal fluctuations.

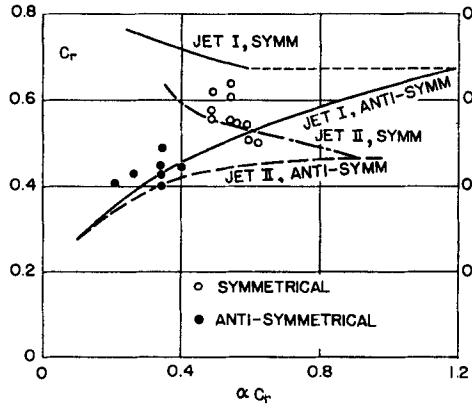

FIGURE 30. Propagation velocity c_r.

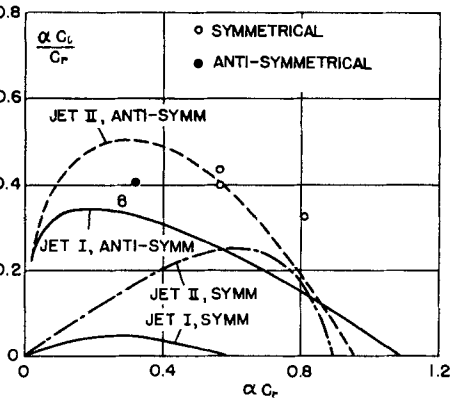

FIGURE 31. Spatial rate of amplification $\alpha c_r/c_i$.

The distribution of amplitude is shown in figure 32, taking the maximum value as unity. The experimental points are root-mean-square values of spectral components of u-fluctuations without artificial excitations. The theoretical curves are those of amplified oscillation based on Jet II with approximately maximum spatial rate of amplification. The agreement between experimental and theoretical results is satisfactory except near $y = 1$ for the symmetrical fluctuation. This disagreement may arise from the slight misfit of assumed basic flow (Jet II) to experimental distribution, because the theoretical amplitude function is extremely sensitive to the mean-velocity distribution as well as its derivatives.

From the preceding discussion, it is concluded that in the two-dimensional jet there is a region in which the velocity fluctuation field is well described by the linearized Navier–Stokes equations. Moreover, considering that the separated layer is an extreme case of a jet, a more general treatment of both flows is possible as shown by the present author (1959).

The regular pattern of sinusoidal fluctuations in a jet suggests a comparison of it with the laminar-boundary-layer oscillations in a boundary layer and the double row of vortices behind a cylinder.

Sinusoidal fluctuations in the free boundary layer seem to be essentially the same as those oscillations found by Schubauer & Skramstad in the boundary layer along a flat plate, except for two remarkable differences. One is the frequency of naturally excited oscillations. In the case of the boundary layer along a plate, the frequency lies on the second branch of the neutral curve as illustrated schematically in figure 33. This is a rather curious situation, because along the

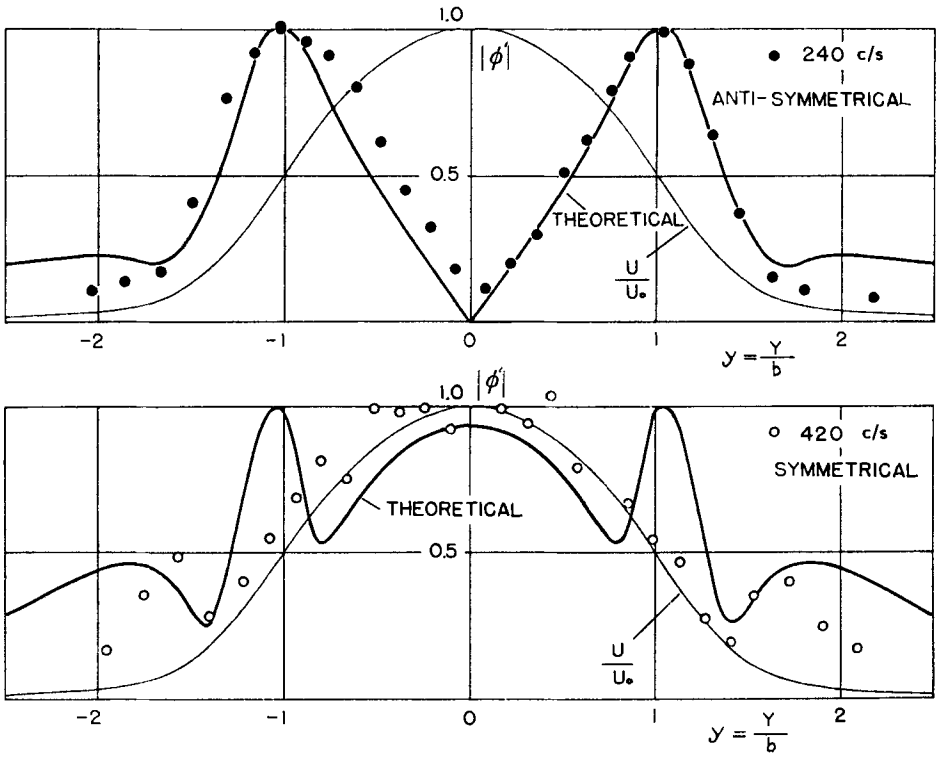

FIGURE 32. Amplitude function. In theoretical results, parabolic distribution (distribution II) is used. For anti-symmetrical fluctuations, $\alpha = 0{\cdot}62$, $c_i = 0{\cdot}28$ and for symmetrical fluctuation, $\alpha = 0{\cdot}88$, $c_i = 0{\cdot}142$.

neutral curve no fluctuation is supposed to be amplified. The explanation for this was given by Schubauer & Skramstad. According to their description, the velocity fluctuation with a definite frequency is amplified along a horizontal line inside the amplified zone in figure 33; and for given Reynolds number R_1, for instance, the frequency which receives maximum amplification lies just inside the amplified zone near branch II. Therefore, the frequency of naturally excited oscillation is found near branch II of the neutral curve.

The situation in the jet is quite different. Since the jet is created by the liberation of channel flow, its history does not begin at $R = 0$. The layer starts suddenly at R_0, for instance, and intensity of sinusoidal fluctuation reaches the *linearity limit* at R_1, which is not so much different from R_0 because of the great rate of amplification in the jet. Therefore, the frequency which receives maximum amplification lies approximately along a line of maximum amplification at R_0 or R_1. In other words, oscillations in the boundary layer along a plate are amplified

over a long history; on the contrary, the fluctuations in a jet are amplified in an instant. This is relevant to the difference in the rate of amplification, which is the second point of difference between these two kinds of fluctuation. The rate of amplification of fluctuations in a jet is roughly 10 times of that in a boundary layer along a plate. The development of velocity fluctuation in the 'non-linear' region may also be influenced by this great difference in the rate of amplification between 'fixed' and free boundary layers.

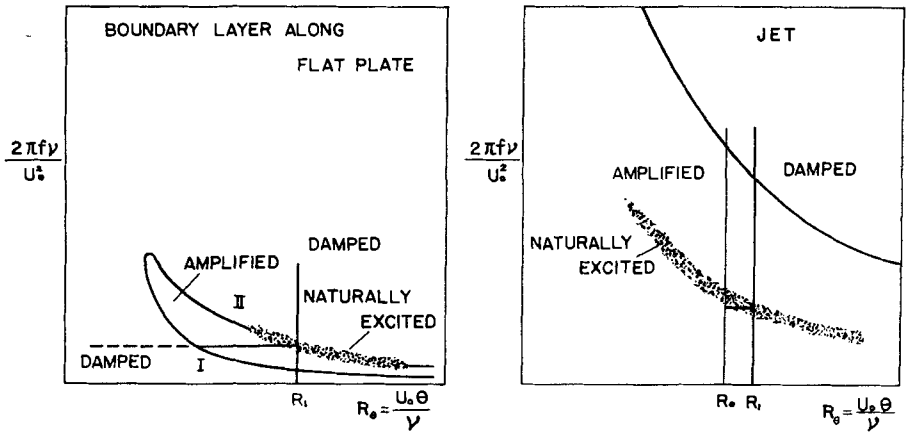

FIGURE 33. Schematic diagrams of amplified zones in the boundary layer along a flat plate and jet.

The vortex street formed in the wake behind a two-dimensional body seems to be essentially different from sinusoidal fluctuations in the jet. When we compare the fluctuations in jet and wake of cylinder we notice, at first, that the energy of sinusoidal fluctuations in the wake is far greater than that in the jet. The maximum root-mean-square intensity $(\overline{u^2})^{\frac{1}{2}}_{\max}/U_0$ of fluctuations in a wake reaches 0·16 according to the measurement by Roshko (1953). The value is approximately 4 times of that found in the jet. It is inconceivable that the fluctuation of such a high intensity as observed in the wake could be treated by linearized theory, unless there is a certain cause which suppresses the non-linear effect.

Another difference between the jet and wake is concerned with the growth of fluctuations. The sinusoidal fluctuation in the wake is usually decaying and no exponential growth has been observed so far. The mechanism of generating sinusoidal fluctuation in the wake is complicated since it seems to be associated with the periodical movement of separation point or stagnation point on the cylinder. At the present stage of knowledge, it seems to be impossible to treat the fluctuations in both jet and wake of a cylinder on a common basis.

5.4. *Transition region*

Generally speaking, the physical process taking place in the transition region of a jet is very similar to that of a separated layer. Especially when the slit is wide, the structure of the transition region of a jet is exactly the same as that of a separated layer. In other words, the shear layer at one side of a jet does not know the existence of the shear layer at the other side. In this case, the mean-

velocity distribution has a wide, flat core at the central part, and the two shear layers from the two sides meet after they become turbulent. In the present experiment, transition of this type is observed when $\nu l/h^2 U_{00}$ is smaller than about 0·015. For larger values of $\nu l/h^2 U_{00}$, the interaction of both shear layers becomes remarkable. Figure 11 shows the development of intensity of velocity fluctuations along the centre line in such a case. The linearity limit is about $(\overline{u_0^2})^{\frac{1}{2}}/U_{00} = 0{\cdot}04$, and the transition point defined by the linearity limit is found at $X/2h \doteqdot 5$–7. The intensity reaches a maximum at about $X/2h = 12$ and begins to decrease thereafter. The structural equilibrium in turbulent jet seems to be accomplished at $X/2h \doteqdot 30$–40.

Two non-dimensional quantities concerning mean velocity, $(U_{00}/U_0)^2$ and b/h, are, roughly speaking, proportional to $X/2h$ in the transition region, although other kinds of expression are also possible from the experimental data (figures 3 and 4). It is interesting to note that the proportionality relations hold in the fully turbulent jet (Townsend 1956). The transition point determined by the spread of jet is in good agreement with that determined by the linearity limit of intensity of u-fluctuations.

From the mean-velocity survey, the mean streamlines were determined experimentally. We notice that the two dividing streamlines—streamlines which start from the edge of the slit—shrink slightly at about $X/2h = 8$, when $U_{00} = 10{\cdot}0$ m/s with SLIT 6 mm L. They, of course, diverge as the distance downstream is further increased. This shrinkage of streamlines means an acceleration of the flow, which results in a decrease of static pressure there. In fact, the static-pressure distribution along the centre line measured under the same conditions shows a minimum at about $X/2h = 8$. The static pressure there is lower than that of the surrounding atmosphere by about 15 % of the dynamic pressure $\frac{1}{2}\rho U_{00}^2$. On the other hand, in the laminar layer and fully turbulent region, the difference of pressure is at most 2 % of the dynamic pressure. These peculiar features of streamlines and static pressure in the transition region might have some relations to the development of velocity fluctuations. But at present detailed relations are not known.

Concerning fluctuation patterns in the transition region of jet, no concrete conclusion is drawn except the non-existence of intermittent burst. The waveform of the u-fluctuations changes gradually from sinusoidal to the irregular pattern which is characteristic of turbulent flow. In the energy spectrum, peaks at definite frequency, which correspond to symmetrical and anti-symmetrical sinusoidal fluctuations, become lower and lower continuously, distributing the energy to other spectral components.

The classification of the transition region as shown in figure 11 is possible also in the case of a boundary layer along a flat plate. Figure 34 is a plot of the maximum intensity of u-fluctuations in each X-station against X. The data were taken from the experiment conducted by Schubauer & Klebanoff (1956) in the boundary layer on a flat plate. The linearity limit is apparently observed at about $(\overline{u^2})^{\frac{1}{2}}_{\max}/U_0 = 0{\cdot}06$. The variation of intermittency factor in the X-direction indicates that the transition point defined by the linearity limit corresponds approximately to the beginning of intermittent bursts. As shown in figure 34, the non-linear region starts at the linearity limit and ends when the intermittency factor

reaches 1. A classification of this kind into linear region, non-linear region and fully turbulent region may be possible for all flows which include transition.

On the possible cause of intermittent burst in the transition region, only conjectures have been made so far by many investigators. In the two-dimensional jet, no intermittent burst was found. The definition of 'burst' itself is so vague that one might call any instantaneous increase of amplitude of fluctuation a 'burst'. Regardless of the difference in definition, the burst in the free boundary layer is, at least, much less remarkable than that observed in the boundary layer

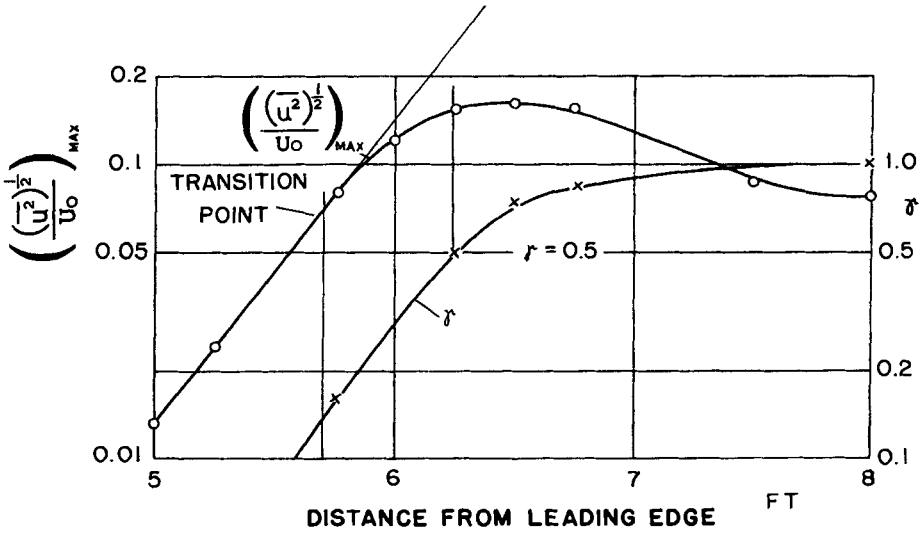

FIGURE 34. Logarithmic plot of maximum intensity of velocity fluctuation in boundary layer along a flat plate. Data after Schubauer & Klebanoff (1956).

on a plate. The reason why there are no bursts in the free boundary layer is not apparent, but it is mentioned with certainty that the generation of a burst is connected with the stability characteristics of the flow as well as with the difference of mean-velocity distribution of laminar and turbulent layers. First, neutral curves, for instance, of a jet and a boundary layer on a flat plate are different, as shown in figure 33. In the boundary layer on a plate, a velocity fluctuation at a certain wave-number is amplified only between the first and second branch of the neutral curve; while in the jet, fluctuation is amplified without limitations.

Concerning the mean-velocity distribution, distributions of laminar and turbulent layers are quite different in a boundary layer on a plate and in pipe flows. Therefore, if the rapid transition between these two states of mean-velocity distribution is required for the energy equilibrium in the layer, the 'fly-back' in mean-velocity distribution can be a cause of intermittent burst. In fact, Rotta (1956) has shown a close relationship between the intermittent burst and mean velocity. The presence of a solid wall in the flow can be another cause of complication in transition. It has various effects on the formation and development of two- or three-dimensional waves or vortices.

When free boundary layers are excited artificially, the above considerations

are enough when the intensity of excitation is low. With increased intensity of excitation, the amplitude of velocity fluctuation 'overshoots' as shown in figure 18. In this case, the velocity fluctuation rearranges itself, possibly by non-linear interactions, until certain equilibrium is reached. The wave-form becomes peculiar when the level of excitation is high.

The quantitative discussion in the transition region is still hardly possible. More systematic and extensive experiments are needed to understand details of Reynolds stresses, pressure fluctuations, dissipation terms and spectral components of u, v and w.

Theoretical investigations should be made parallel with experiments, considering the three-dimensional nature of velocity fluctuations, non-linear terms and viscous dissipation, and using the solution in the linear region as initial condition.

6. Conclusion

From the experimental and theoretical investigations concerning two-dimensional jet, the following conclusions have been obtained:

1. The similar mean-velocity distribution of a laminar jet was not established under the present experimental conditions.

2. When the slit is narrow, the frequency of sinusoidal fluctuations in the jet is almost proportional to the speed of the jet. When the frequency is non-dimensionalized by taking the maximum speed and the momentum thickness of layer as units, it is constant over a wide region of Reynolds number.

3. The sinusoidal fluctuations are similar to the oscillations found in a laminar boundary layer on a flat plate and dissimilar to the double row of vortices in the wake of a cylinder.

4. When the amplitude of sinusoidal fluctuations is not large, it grows exponentially. The frequency, propagation velocity, rate of amplification and amplitude function of fluctuation show good agreement with the predictions of linearized theory.

5. A distinct physical meaning can be given to the 'transition point' by defining it as a point where the growth rate of intensity of velocity fluctuation deviates from being exponential.

6. No intermittent bursts were found in the transition region.

7. The separated layer may be considered as an extreme case of a jet. Both flows belong to the 'jet-type boundary layer'.

The author appreciates the stimulating discussions and advice given throughout the whole course of the investigation by members of the Turbulence Research Group in Japan, which is directed by Professor Itiro Tani. Thanks are extended to Messrs Y. Onda and S. Kyoya who helped to carry out the experimental work, and to Miss M. Nakagawa who assisted in the numerical calculations. This work was financially supported by the Scientific Research Fund of the Ministry of Education of Japan.

REFERENCES

ANDRADE, E. N. DA C. 1939 *Proc. Phys. Soc.* **51**, 784.

BROWN, G. B. 1935 *Proc. Phys. Soc.* **47**, 703.

FÖRTHMANN, E. 1934 *Ingen.-Arch.* **5**, 42.

LESSEN, M. & FOX, J. A. 1955 50 *Jahre Grenzschichtforschung*, p. 122.

ROSHKO, A. 1953 *Nat. Adv. Comm. Aero., Wash., Tech. Note* no. 2913.

ROTTA, J. 1956 *Ingen.-Arch.* **24**, 258.

SATO, H., KOBASHI, Y., IUCHI, M., YAMAMOTO, K. & ONDA, Y. 1954 *Rep. Inst. Sci. Tech. Univ. Tokyo*, **8**, 271.

SATO, H. 1956 *J. Phys. Soc. Japan*, **11**, 702.

SATO, H. 1957 *Rep. Inst. Sci. Tech. Univ. Tokyo*, **11**, 73.

SATO, H. 1959 *Rep. Aero. Res. Inst. Univ. Tokyo* (to be published).

SAVIC, P. 1941 *Phil. Mag.* **32**, 245.

SCHLICHTING, H. 1934 *Z. angew. Math. Mech.* **14**, 368.

SCHUBAUER, G. B. & SKRAMSTAD, H. K. 1948 *Nat. Adv. Comm. Aero., Wash., Rep.* no. 909.

SCHUBAUER, G. B. & KLEBANOFF, P. S. 1956 *Nat. Adv. Comm. Aero., Wash., Rep.* no. 1289.

TATSUMI, T. & KAKUTANI, T. 1958 *J. Fluid Mech.* **4**, 261.

TOWNSEND, A. A. 1956 *The Structure of Turbulent Shear Flow*, p. 192. Cambridge University Press.

WEHRMANN, O. & WILLE, R. 1957 *Proc. Boundary Layer Symposium, Freiburg*, p. 387.

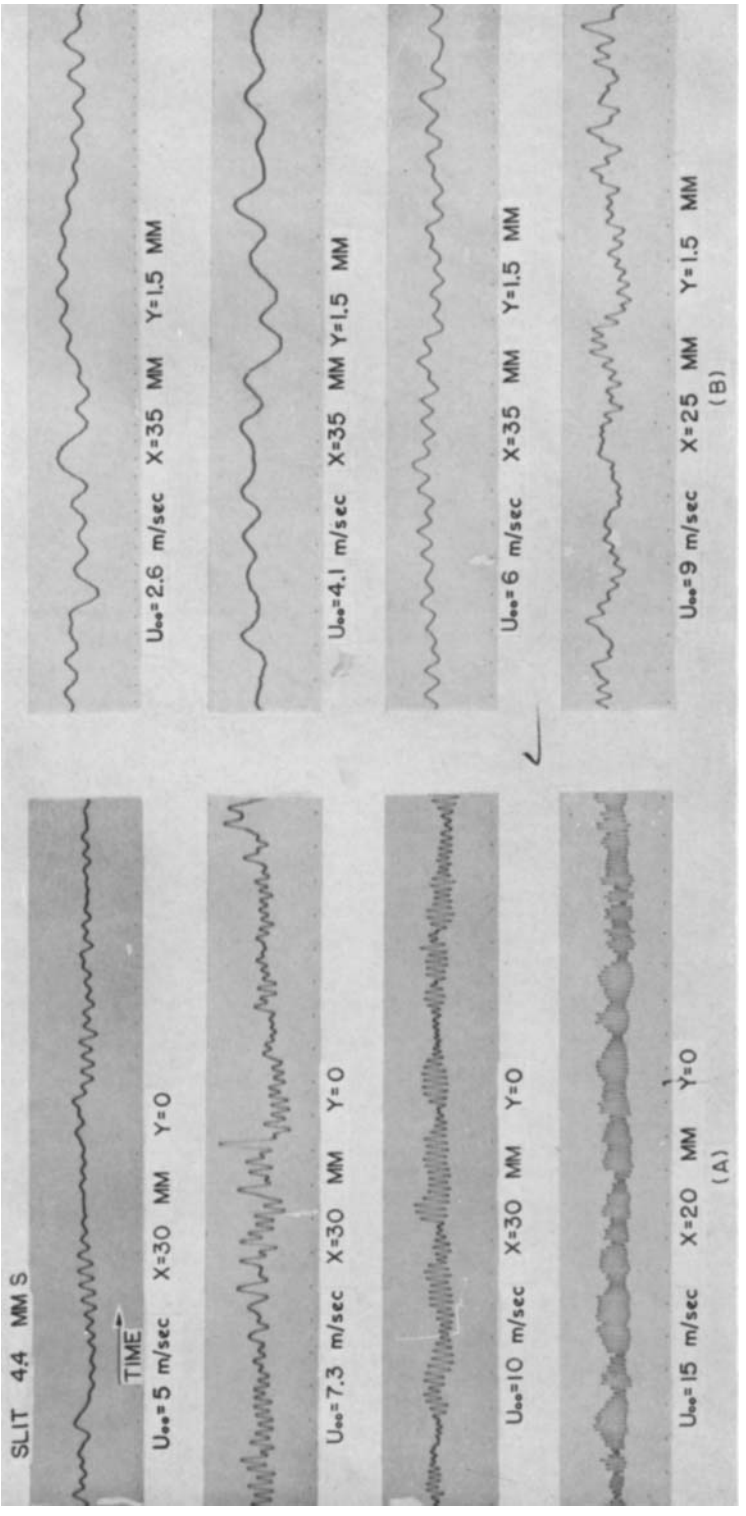

FIGURE 5. Oscillographic records of u-fluctuations. Time interval between dots is 0·01 sec.

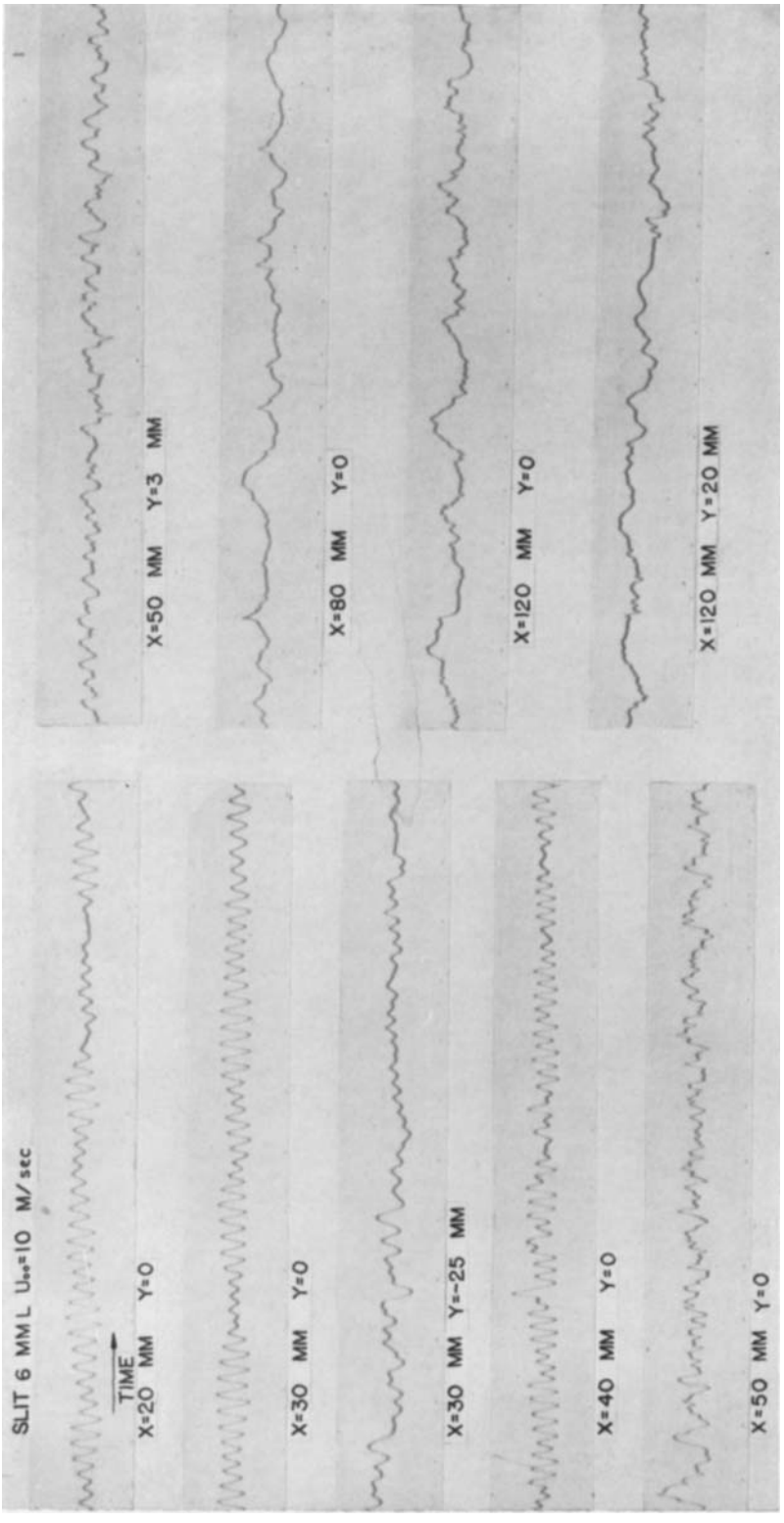

FIGURE 9. Development of u-fluctuations. Time interval between dots is 0·01 sec.

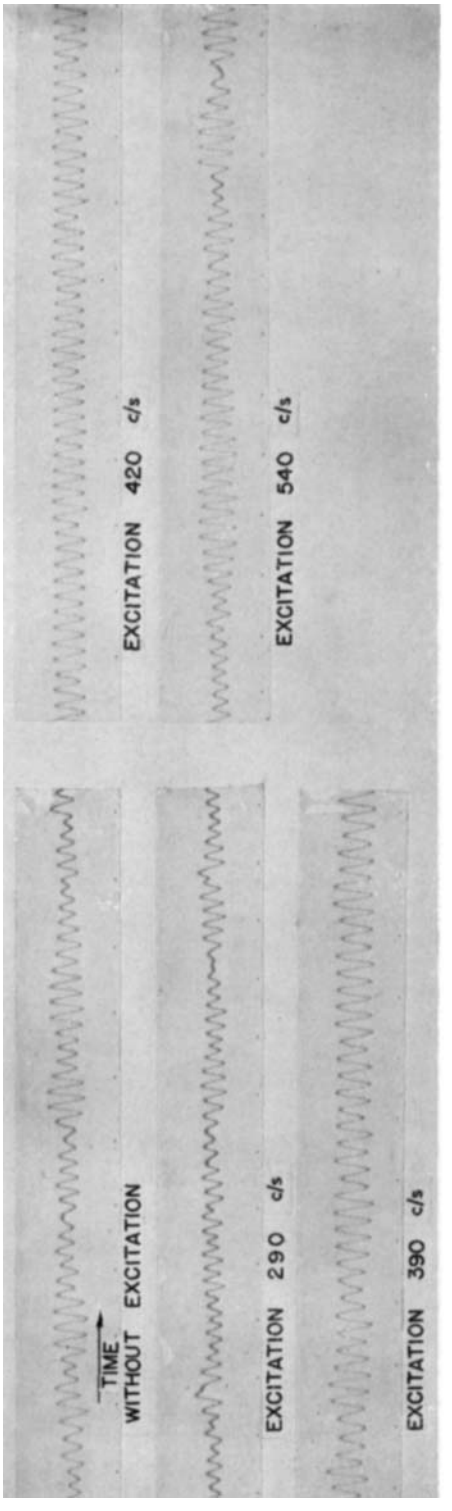

FIGURE 12. Effect of excitation by sound on wave-forms of u-fluctuations. SLIT 6 mm L, $U_{00} = 10{\cdot}0$ m/sec.

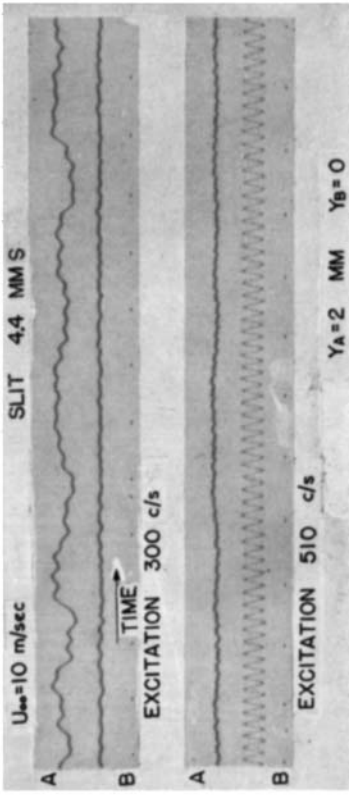

FIGURE 14. Simultaneous records of u-fluctuations at $Y = 0$ and $Y = 2$ mm. SLIT 4·4 mm S. $U_{00} = 10{\cdot}0$ m/sec, $X = 20$ mm.

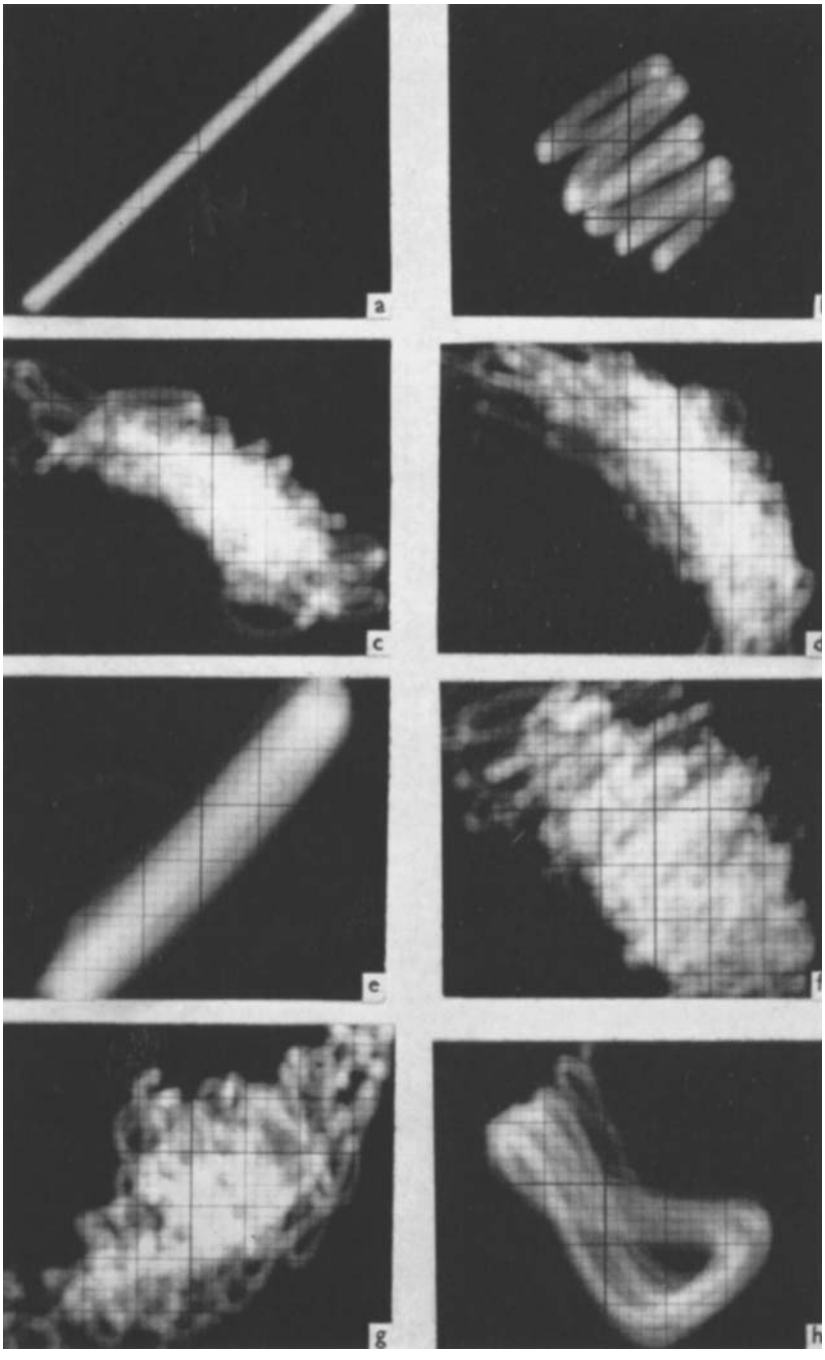

FIGURE 15. Lissajous figures of signals from two hot-wires placed apart in Y-direction. SLIT 6 mm L, $U_{00} = 10{\cdot}0$ m/sec, $X = 30$ mm. (*a*) Standard signals in the same phase. (*b*) $Y = \pm 1$ mm, without excitation. (*c*) $Y = \pm 1$ mm, excitation 240 c/s. (*d*) $Y = \pm 1$ mm, excitation 330 c/s. (*e*) $Y = \pm 1$ mm, excitation 420 c/s. (*f*) $Y = \pm 1$ mm, excitation 600 c/s. (*g*) $Y = 2$ mm, 4 mm, excitation 240 c/s. (*h*) $Y = 2$ mm, 4 mm, excitation 420 c/s.